Theor Chem Acc (2007) 118:99–106
DOI 10.1007/s00214-007-0251-4

REGULAR ARTICLE

Nonlinear optical properties of C_{60} with explicit time-dependent electron dynamics

Garth A. Jones · Angela Acocella · Francesco Zerbetto

Received: 24 November 2006 / Accepted: 13 December 2006 / Published online: 3 February 2007

Abstract An explicit electron dynamics approach has been used to calculate the nonlinear optical properties of C_{60} and its radical anion. An external perturbation, in the form of an oscillating electric field, induces the time-evolution of the molecular wavefunction. The time-averaged instantaneous dipole moment of the systems gives the molecular response to perturbations of varying field intensities and frequency of oscillation. The polarizabilities and the second-order hyperpolarizabilities have been calculated and are in good qualitative agreement with experimentally available data. In line with previous theoretical and experimental studies, the nonlinear effect is enhanced for the radical species.

Keywords Time propagation · Nonlinear optical properties · Fullerenes · Polarizabilities

Introduction

Extended π-electron conjugated systems of carbon atoms have a number of features that make them appealing for practical applications, which many traditional, technologically exploited, inorganic materials do not have. These include ultrafast response times upon exposure to the electromagnetic radiation, low dielectric constants, good processability characteristics, and an enhanced nonlinear optical response, NLO [1,2]. CH-bonds usually have a detrimental effect on NLO responses and therefore pure carbon systems, such as fullerenes, appear good candidates for the exploitation of nonlinear optical properties. C_{60}, the smallest fullerene produced in sizable quantities, has been investigated both experimentally and theoretically together with its higher isomers [3–23]. The various experimental investigations involved measurements by a variety of techniques that resulted in a spread of values. Many of the calculations of the second hyperpolarizability of C_{60} were based on semiempirical and local density (LDA) approaches. These calculations also produced a range of data, which encompasses two orders of magnitude. The wealth of experimental and theoretical data available for the NLO properties of C_{60} makes it an interesting system to test the application of electron dynamics approaches for modelling NLO effects. Here, we apply to this problem an explicit electron dynamics method, where the time-dependence is built into the perturbed part of the Hamiltonian operator via an external oscillating electric field [24]. Application of the electric field induces electron density flow inside the molecule, which, in turn, results either in polarization effects or even in electronic transitions between the molecular orbitals. The method was recently applied to wavefunctions calculated using the B3LYP (hybrid) density functional and showed that a simple 4-electrons molecule, LiH, undergoes population inversion between the HOMO and the LUMO when the electric field is in resonance with the HOMO–LUMO energy gap. It was also shown that the magnitude of the electric field directly affects the rates at which the charges between the atoms oscillate and the rates at which the electronic transitions occur. The model also detected monochromatic and bichromatic multiphoton transitions in the form of one-, two- and three-photon transitions, which could be step-wise.

Contribution to the Fernando Bernardi Memorial Issue.

G. A. Jones · A. Acocella · F. Zerbetto (✉)
Dipartimento di Chimica, G. Ciamician,
Università di Bologna, V. F. Selmi 2, 40126 Bologna, Italy
e-mail: francesco.zerbetto@unibo.it

After presenting the computational scheme for the calculations, we give an overview of past experimental and computational results for C_{60} and compare these results to our own. All the calculations reported are microscopic in nature and no attempt is made to turn them into their macroscopic counterparts.

Computational details

In this work, we model the electron dynamics of C_{60} subject to several external electric fields. The time-dependent algorithm employs the propagator proposed by Allen and coworkers, [25–28] which reads:

$$\Psi(t+\Delta t) = \left(1+\frac{iH\Delta t}{2\mathrm{h}}\right)^{-1}\left(1-\frac{iH\Delta t}{2\mathrm{h}}\right)\Psi(t) \tag{1}$$

where Ψ is the electronic wavefunction; H is the Hamiltonian matrix, given by the sum of the unperturbed molecular Hamiltonian, H^0, and the perturbing Hamiltonian, H', given by the interaction between the classical electric field and the molecular dipole moments; and Δt is the timestep, here set to 0.4 atomic units or 0.0098 fs. The nuclear geometry is frozen during the dynamics and possible electronic transitions, together with the polarization of the molecule, take place as a consequence of the application of the external electric field.

The initial wavefunction $\Psi(t=0)$ and the Hamiltonian H^0 are obtained with the Gaussian03 suite of programs at the B3LYP/6-31G* level [29]. The perturbing Hamiltonian, H', is the product of the matrix of the dipole moments in the atomic basis, D, calculated along the direction of the applied electric field and a sinusoidal wave of the oscillating external field, F:

$$H'(t) = -DF(t)\sin(\omega t) \tag{2}$$

where ω is the frequency of the field. The field amplitude, F, is constant here, but may change in time.

The molecular coefficients are updated at each time step because of the effect of the external perturbation. The time evolution of the atomic orbitals coefficients under the influence of the oscillating field allows us to monitor the electronic occupations of the molecular orbitals in time, in terms of the one-electron density matrix P. At each step, we are able to evaluate the instantaneous dipole moment of the molecule as:

$$\langle\mu(t_i)\rangle = \sum\nolimits_{\alpha} Z_\alpha \boldsymbol{R}_\alpha - \mathrm{tr}(DP(t_i)) \tag{3}$$

where: Z_α and $\boldsymbol{R}_\alpha$ are the nuclear charges and coordinates, D the dipole moment matrix and tr stands for the trace of the matrix in brackets.

For the analysis, one can write the dipole moment in terms of polarizability and hyperpolarizabilities as a function of the field, E:

$$\mu_i = \mu_i^0 + \sum_j \alpha_{i,j}E_j + \frac{1}{2}\sum_{jk}\beta_{ijk}E_jE_k + \frac{1}{6}\sum_{jkl}\gamma_{ijkl}E_jE_kE_l + \cdots \tag{4}$$

where i, j, k, l are the Cartesian axes. Calculation of the dipole moment at several fields, and subsequent interpolation of its values give a polynomial function. The first derivative is proportional to the molecular polarizability, whereas the third derivative is proportional to the second-order hyperpolarizability. Notice that in C_{60}, both μ_0 and β are zero by symmetry and this constrain must be satisfied when evaluating $\langle\mu(F)\rangle$.

Alternatively, the introduction of an electric field, modifies the energy of the system, that can be evaluated at zero field as a Taylor expansion:

$$E(F) = E + \left(\frac{\mathrm{d}E}{\mathrm{d}F_\alpha}\right)F_a + \frac{1}{2!}\left(\frac{\mathrm{d}^2E}{\mathrm{d}{F_\alpha}^2}\right)F_aF_b + \frac{1}{3!}\left(\frac{\mathrm{d}^3E}{\mathrm{d}{F_\alpha}^3}\right)F_aF_bF_c + \frac{1}{4!}\left(\frac{\mathrm{d}^4E}{\mathrm{d}{F_\alpha}^4}\right)F_aF_bF_cF_d + \cdots \tag{5}$$

where a, b, c, d are Cartesian axes. Equation 5 is the basis of the standard quantum chemical approaches, employed also in the Gaussian program, to calculate the polarizability, α, the first hyperpolarizability, β, and the second hyperpolarizability, γ.

Our approach is similar to that proposed by Schlegel and coworkers [30,31] and does not include electron correlation and or spin–orbit interaction terms.

Results and discussion

In this work, we simulate the main NLO property of C_{60}, that is, its second-order hyperpolarizability, γ. Experimentally, γ, is measured by a variety of techniques. Here, we consider third harmonic generation, THG, experiments that give $\gamma(-3\omega;\omega,\omega,\omega)$, which is related to the ability of a molecule to scatter a single photon with the energy of three incoming photons and degenerate four wave mixing, DFWM, experiments that give $\gamma(-\omega;-\omega,\omega,\omega)$, which is related to holography when obtained by optical phase conjugation [32].

Table 1 Experimental C_{60} third-order optical susceptibility, $\chi^{(3)}$ in esu, and calculated second-order hyperpolarizability, γ, in esu

Experimental			Calculated			
$\lambda(\mu m)$	$\chi^{(3)}\times 10^{11}$	Technique	$\lambda(\mu m)$	$\gamma\times 10^{34}$	Technique	Method
0.60	22	DFWM[6]	0	2.041	THG	SOS-VEH[4]
0.63	30	DFWM[12]	0	0.0495		INDO-TDCPHF[6]
0.85	1.5	THG[17]	1.37	0.0504	OKG	INDO-TDCPHF[6]
1.06	0.7	DFWM[9]	1.37	0.0549	EFISH	INDO-TDCPHF[6]
	1.4	THG[10]	1.37	0.0552	DFWM	INDO-TDCPHF[6]
	7.2	THG[20]	0	0.0239		MNDO-PM[37]
	8.2	THG[17]	0	0.0159		LDA[8]
	20	THG[11]	1.064	8.84	DFWM	SOS-INDO/S[11]
1.32	3.	THG[10]	1.91	6.9	DFWM	SOS-INDO/S[11]
	6.1	THG[17]	0	0.07		LDA[13]
1.50	3.0	THG[20]	0	0.09		TB[14]
1.91	0.9	THG[10]	0	4.58		SOS-CNDO/S[22]
	1.6	EFISH[5]	0	1.34		SOS-CNDO/S[23]
	3.2	THG[17]				
2.00	3.7	THG[20]				
2.37	0.4	THG[10]				

OKG optical Kerr gate; *EFISH* electric field induced second harmonic generation

Summary of previous results

Before presenting the results, it is convenient to assess the experimental and theoretical results known to date for C_{60}. Table 1 presents such a summary. Notice that it is not within the scope of this work to investigate the relation between macroscopic. i.e. experimental, and microscopic, i.e. calculated, polarizabilities. For sake of comparison, we can assume that a factor of 10^{22}–10^{23} relates theory and experiment [33,34].

By inspection of Table 1, several features become apparent:

(i) the experimental results are scattered,
(ii) the third-order optical susceptibility of C_{60} is larger than 10^{-11} esu,
(iii) the experimental values are better reproduced by Sum-Over-States, SOS, type of calculations rather than by the coupled Hartree–Fock approach.

While, there may be various reasons for the inaccuracy of the methods based on a perturbative expansion of the energy (perhaps the most likely is connected with the very low S_0–S_1 energy gap in fullerenes) the need for another approach emerges.

C_{60} radical anion has been less investigated [35,36]. The authors used their experimental data to obtain a value for the microscopic second hyperpolarizability of $\gamma(C_{60}^-) = 2.4 \times 10^{-33}$ esu, which is larger than what obtained for neutral C_{60} by up to about an order of magnitude.

Dipole moment dynamics

Figure 1 provides two illustrative examples of the dynamics of the dipole moments over ∼6 fs for the propagation of the electronic wavefunction of C_{60} upon switching on the electric field perturbation. The field intensity was set to 0.005 or to 0.01 atomic units, which are equal to 0.257 V Å^{-1} or to 0.514 V Å^{-1}. These values are substantial and must not be taken as those experienced by the molecule under laser irradiation in the measurements of the nonlinear optical response. The range of the fields used in the calculations is related to the necessity of having a stable third derivative of the dipole moment as a function of the electric field, $\mu(F)$. In any event, one should notice that the largest value of the field used here, 0.01 atomic units, is smaller than what is typical of a variety of applications in practical devices, such as for instance in field effect transistors, where the gate generates an electric field that can be several times larger. As expected, Fig. 1, shows that with the larger field, on the right, there is a greater molecular response.

The figure pictorially shows a practical issue that must be taken into account when calculating $<\mu>_t$: owing to the periodicity of the response, the average value of the dipole moment, at any given field, must be calculated over a time that corresponds to a multiple of a 2π rotation of the field. This varies slightly as a function of the frequency of the field and is not the same for all the calculations that have been performed. In the cases of Fig. 1, a 2π rotation is accomplished in slightly more than 5 fs.

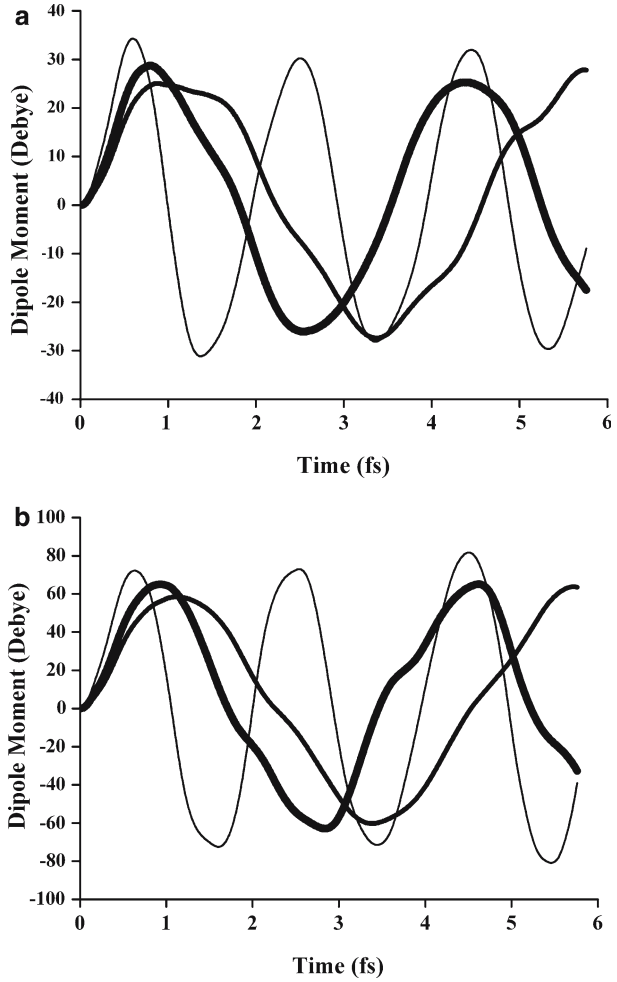

Fig. 1 Time dependence of the instantaneous dipole moment for neutral C_{60}. The wavelengths are 1.064 μm (*thick line*), 1.37 μm (*medium thickness line*) and 0.60 μm (*thin line*). The field intensity is **a** 0.005 atomic units equal to 0.257 V Å^{-1}; **b** 0.01 atomic units equal to 0.514 V Å^{-1}

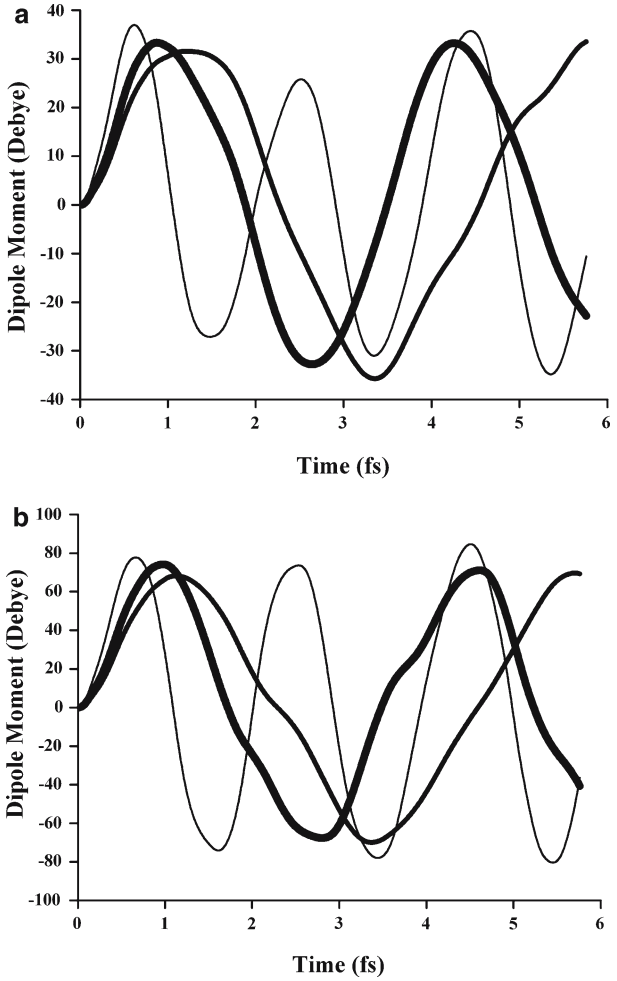

Fig. 2 Time dependence of the instantaneous dipole moment for radical anionic C_{60}. The wavelengths are 1.064 μm (*thick line*), 1.37 μm (*medium thickness line*) and 0.60 μm (*thin line*). The field intensity is **a** 0.005 atomic units equal to 0.257 V Å^{-1}; **b** 0.01 atomic units equal to 0.514 V Å^{-1}

Figure 2 shows the instantaneous dipole moment at the same fields for C_{60} radical anion. The addition of an extra electron only weakly affects the instantaneous response of the dipole moment, although as it becomes apparent below, such weak variations ultimately results in a variation of the second order hyperpolarizability.

Field dependent dipole moment

In agreement with the data of Figs. 1 and 2, the curves of Fig. 3 show that the average dipole moments of the two species do not differ greatly. For neutral C_{60}, the deviation from linearity is small. The higher terms become larger when an extra electron is present.

The fittings of the data were carried out selecting two maximal values for the field. The lower value of 0.257 V Å^{-1} eliminates the majority of the higher order terms. The higher value of 0.514 V Å^{-1} includes them.

Table 2 shows the results. The first term is the polarizability, α, the second is the second hyperpolarizability, γ. The dipole moment is in Debyes so that the units are $[\alpha] = [C^2\,m^2\,J^{-1}]$ and $[\gamma] = [C^4\,m^4\,J^{-3}]$.

Notice that cgs and MKS electrostatic units also differ by 4π.

A relatively large number of experimental results are also available for the polarizability of C_{60}. The calculated values of polarizability reported in Table 2 range from 37.3 to 59.6 Å^3 (in esu). The corresponding experimental values range from 76.5 to 90.9 Å^3, [37–41] while previous calculations have provided values that range from 36 to 154 Å^3. [42–52]. It should be noticed that most of the experimental data are obtained in the solid phase.

The second hyperpolarizability is the cubic component of the field-dependent dipole moment. In practice, a variety of experiments can provide its macroscopic

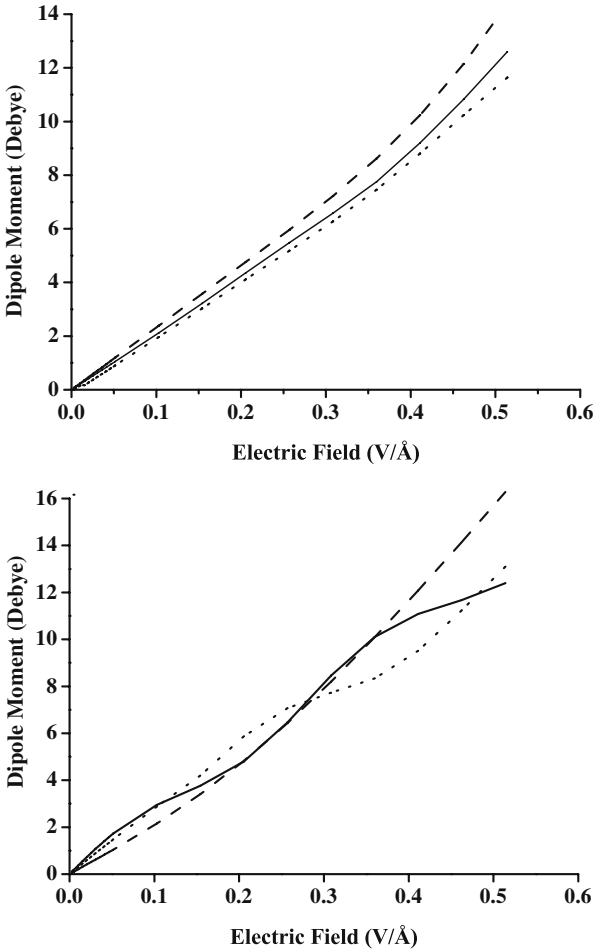

Fig. 3 Dipole moment as a function of the electric field. The wavelengths are 1.064 μm (solid line), at 1.37 μm (dotted line) and at 0.60 μm (dashed line). **a** neutral C_{60}; **b** radical anionic $C_{60}^{\cdot -}$

counterpart. Differences arise because of the nature of the input and output radiation. For instance, in THG a photon with three times the energy of the incoming photons is scattered. On the contrary, in DFWM the scattered photon has the same energy of the interacting incoming photons. In order to qualitatively account for these differences, the numerical functions of Fig. 3 were Fourier-transformed and only the component with the frequency of the outgoing photon was retained for the fittings to Eq. 4, where only the linear and cubic terms are present. Table 3 shows the results of the fittings.

Inspection of the table shows that:

1. The calculated values for neutral C_{60} are comparable to those obtained by the SOS model, which is deemed to better reproduce the experimental results.
2. The field cutoff affects the value of the hyperpolarizability. This is in keeping with the experiments. Indeed, a strong field not only polarizes the molecule but also strips off its electrons.
3. Shorter wavelengths tend to give rise to larger values of the hyperpolarizability, again in agreement with experiments since as the wavelength approaches that of an electronic transition, resonant effects appear.
4. The second hyperpolarizability of the radical anion of C_{60} is larger than that of the neutral species.

The electronic dynamics

Electric field-induced polarization is brought about by the mixing of the molecular orbitals that the molecule possesses when the field is switched off. C_{60} is highly symmetric and its orbitals are highly degenerate. The mixing can occur both within a set of degenerate orbitals, which is irrelevant to polarization, or between sets of orbitals. In order to appraise the inter-orbital contribution, we monitored in time the occupation of four sets of orbitals, namely the five-fold degenerate HOMO-1, the fivefold degenerate HOMO, the threefold degenerate LUMO, and the threefold degenerate LUMO+1. In the case of the radical anion, the LUMO was split between the singly occupied MO, SOMO, and a pair of LUMOs.

Figures 4 and 5 show the variation in time of the occupancy of the highest occupied and lowest unoccupied molecular orbitals. For illustrative purposes the field

Table 2 Fittings of the field-dependent dipole moment with a linear and a cubic term

C_{60}[a]				$C_{60}^{\cdot -}$[a]		
	α	γ	R^2	α	γ	R^2
0.60 μm	7.95×10^{-39}	4.50×10^{-58}	0.999	8.74×10^{-39}	1.53×10^{-58}	0.999
1.064 μm	6.62×10^{-39}	3.27×10^{-58}	0.997	9.16×10^{-39}	2.25×10^{-58}	0.998
1.37 μm	6.05×10^{-39}	2.18×10^{-58}	0.999	7.2×10^{-39}	7.08×10^{-58}	0.983

The correlation coefficients, R^2, are given. $[\alpha] = [C^2\,m^2\,J^{-1}]$ and $[\gamma] = [C^4\,m^4\,J^{-3}]$. The fittings were obtained with the maximum value of electric field of 0.514 V Å^{-1}

[a] Conversion factors. α: 1 atomic unit = 1.64878×10^{-41} $C^2\,m^2\,J^{-1} = 1.48186 \times 10^{-25}$ cm^3 (esu or cgs) = 1.862 Å^3 (MKS); γ:1 atomic unit = 6.23538×10^{-65} $C^4\,m^4\,J^{-3} = 5.03699 \times 10^{-40}$ esu

Table 3 Hyperpolarizabilities in esu for the neutral and the radical anion C_{60}

	C_{60}					
$\lambda(\mu m)$	$0.257\,V Å^{-1}$			$0.514\,V Å^{-1}$		
	DFWM	THG	Total	DFWM	THG	Total
0.60	5.46×10^{-33}	1.31×10^{-33}	0.21×10^{-34}	8.51×10^{-33}	1.66×10^{-33}	4.01×10^{-33}
1.064	2.65×10^{-33}	1.22×10^{-32}	3.62×10^{-33}	2.77×10^{-33}	4.46×10^{-33}	1.21×10^{-33}
1.37	2.80×10^{-33}	1.12×10^{-33}	6.96×10^{-34}	4.8×10^{-33}	7.03×10^{-33}	1.95×10^{-33}
	$C_{60}^{\cdot -}$					
	$0.257\,V Å^{-1}$			$0.514\,V Å^{-1}$		
0.60	3.83×10^{-33}	3.32×10^{-32}	1.28×10^{-32}	3.38×10^{-33}	3.95×10^{-33}	6.30×10^{-33}
1.064	3.30×10^{-33}	1.38×10^{-32}	2.74×10^{-32}	2.91×10^{-33}	4.70×10^{-33}	4.64×10^{-33}
1.37	1.05×10^{-32}	1.18×10^{-32}	1.14×10^{-32}	4.85×10^{-34}	4.97×10^{-33}	1.07×10^{-33}

oscillates at 1.064 μm. Resonant effects, that is electronic transitions, are not present since in no case the occupancy changes by exactly one unit of occupancy. As the field increases, orbital mixing increases, and a higher fraction of electrons move from the degenerate HOMO-1 and HOMO to the degenerate LUMO and LUMO+1. In practice, for a twofold increase of the field, the minimum value of the occupation of the LUMOs of C_{60} goes from ~9.9 to ~9.4. A similar trend is observed for the radical anion. Furthermore notice that the variation of electron occupation is slowly damped in time. This indicates that the wavefunction of the system evolves towards a stationary state.

It is instructive to compare Fig. 4 to Fig. 5. As can be seen in Fig. 3, the perturbed dipole moments of neutral and radical anionic C_{60} are similar. However, the occupancies, which are responsible for the actual values, behave differently. In neutral C_{60}, Fig. 4, HOMO-1, HOMO, and LUMO contribute similarly to the electron dynamics, with the LUMO+1 nearly as active. In radical anionic C_{60}, Fig. 5, the additional electron appears to be very polarizable. This is likely due to the small SOMO–LUMO gap. The occupancy of the SOMO varies markedly in time and just before 3 fs plunges to 0.25, even for the smaller of the two fields discussed here for illustrative purposes. This extra electron also makes the HOMO-1 and HOMO harder and less polarizable, while it lends a softer character to LUMO and LUMO+1. In short, the model shows that the second-order hyperpolarizability of neutral C_{60} and its radical anion have a different origin.

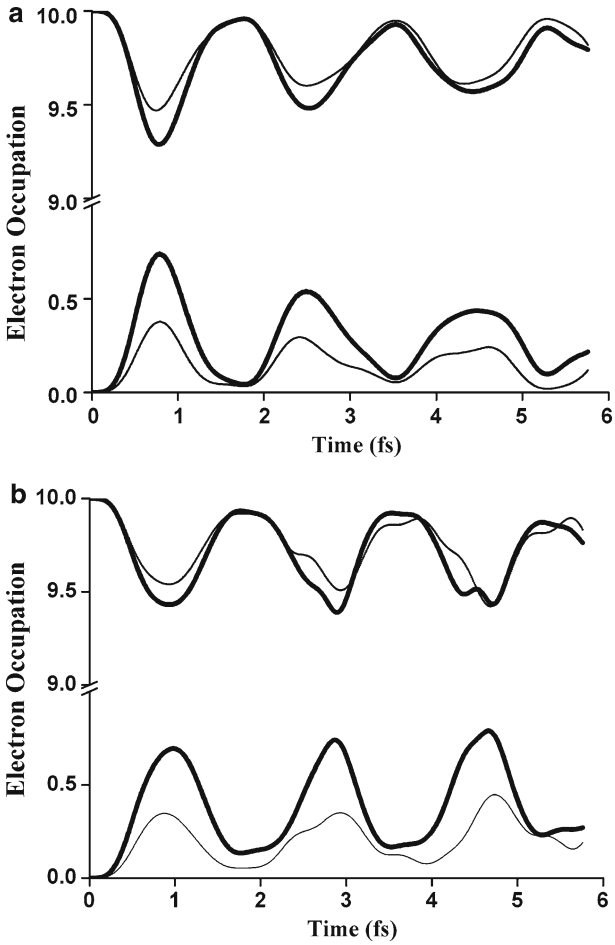

Fig. 4 Time dependent occupation of molecular orbitals of neutral C_{60}. The wavelength of the electric field was set to 1.064 μm. *Top thick line* for HOMO-1; *thin line* for HOMO. *Bottom thick line* for LUMO; *thin line* for LUMO+1. **a** Field intensity $0.257\,V Å^{-1}$; **b** field intensity $0.514\,V Å^{-1}$

Conclusion

An explicit time-dependent model that propagates an electronic wavefunction in the presence of an electric field has been extended to calculate the polarizabilities and is applied to the case of the nonresonant second hyperpolarizability of C_{60}. The calculations are in line

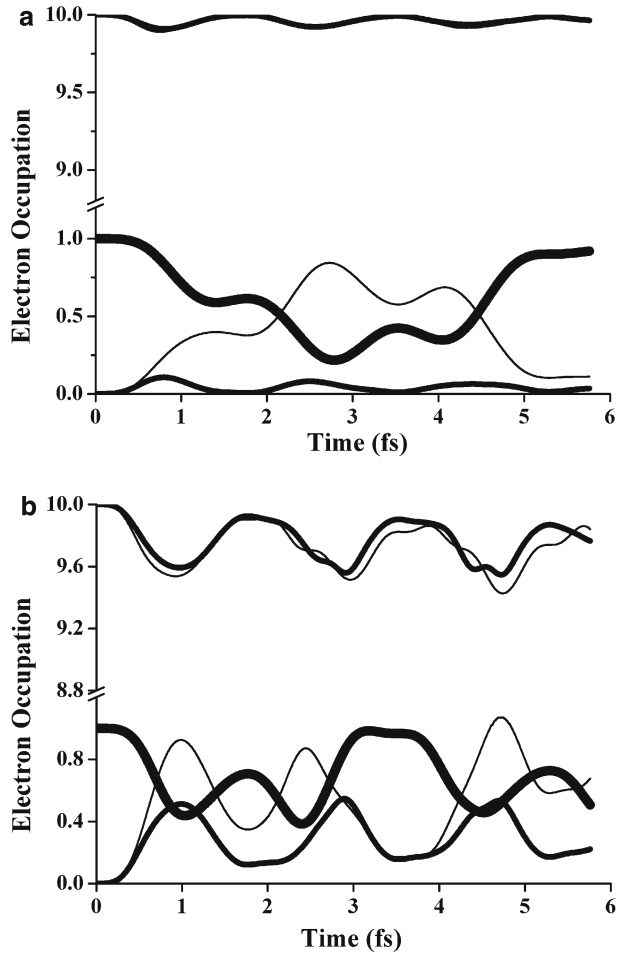

Fig. 5 Time dependent occupation of molecular orbitals of radical anionic C_{60}. The wavelength of the electric field was set to 1.064 μm. *Top thick line* for HOMO-1; *thin line* for HOMO (coincident in the *left figure*). *Bottom* thick line for the two LUMOs; *very thick line* for the SOMO; *thin line* for LUMO+1. **a** Field intensity 0.257 VÅ^{-1}; **b** field intensity 0.514 VÅ^{-1}

with the more accurate results obtained to date and also concur with the experiments where the second-order hyperpolarizability of the radical anion of C_{60} is larger than that of the neutral species. The dynamics of the electron occupancy of the highest occupied and lowest unoccupied molecular orbitals shows that the variation of γ when an extra electron is added to the carbon frame is due to the softness of the SOMO and an additional softness that is introduced for the LUMOs.

Acknowledgements Support from EU programs is gratefully acknowledged.

References

1. Kuyzyk MG, Dirk CW (Eds) (1998) Characterization techniques and tabulations for organic nonlinear optical materials. Marcel Dekker, New York
2. Böttcher CJF (1993) Theory of electric polarization, 2nd edn. In: van Belle OC, Bordewijk P, Rip A (eds). Elsevier, Amsterdam
3. Lindle JR, Pong RGS, Bartoli FJ, Kafafi ZH (1993) Phys Rev B 48:9447
4. Shuai Z, Bredas JL (1992) Phys Rev B 46:16135; ibid. (1993) 48:11520
5. Wang Y, Cheng L-T (1992) J Phys Chem 96:1530
6. Talapatra GB, Manickam N, Samoc M, Orczyk ME, Karna SP, Prasad PN (1992) J Phys Chem 96:5206
7. Matsuzawa N, Dixon DA (1992) J Phys Chem 96:6241
8. Matsuzawa N, Dixon DA (1992) J Phys Chem 96:6872
9. Kafafi ZH, Lindle JR, Pong RGS, Bartoli FJ, Lingg LJ, Milliken J (1992) Chem Phys Lett 188:492
10. Meth JS, Vanherzeele H, Wang Y (1992) Chem Phys Lett 197:26
11. Li J, Feng J, Sun J (1993) Chem Phys Lett 203:560
12. Rosker MJ, Marcy HO, Chang TY, Khoury JT, Hansen K, Whetten RL (1992) Chem Phys Lett 196:427
13. Quong AA, Pederson MR (1992) Phys Rev B 46:12906
14. Wang Y, Bertsch GF, Tomanek DZ (1993) Phys D 25:181
15. Ji W, Tang SH, Xu GQ, Chan HSO, Ng SC, Ng WW (1993) J Appl Phys 74:3669
16. Harigaya K, Abe S (1992) Jpn J Appl Phys 3:L235R
17. Kajzar F, Taliani C, Danieli R, Rossini S, Zamboni R (1994) Chem Phys Lett 217:418
18. Kajzar F, Taliani C, Danieli R, Rossini S, Zamboni R (1994) Phys Rev Lett 73:1617
19. Hoshi H, Nakamura N, Maruyama Y, Nakagawa T, Suzuki S, Shiromaru H, Achiba Y (1991) Jpn J Appl Phys 31:L1397
20. Neher D, Stegeman GI, Tinker FA, Peyghambarian N (1992) Opt Lett 17:1491
21. Yang S-C, Gong Q, Xia Z, Zou YH, Wu YQ, Qiang D, Sun YL, Gu ZN (1992) Appl Phys B 55:51
22. Fanti G, Orlandi G, Zerbetto F (1995) J Am Chem Soc 117:6101
23. Nomura Y, Miyamoto T, Hara T, Narita S, Shibuya T (2000) J Chem Phys 112:6603
24. Acocella A, Jones GA, Zerbetto F (2006) J Phys Chem A 110:5164
25. Allen RE (1994) Phys Rev B 50:18629
26. Graves JS, Allen RE (1998) Phys Rev B 58:13627
27. Torralva BR, Allen RE (2002) J Mol Opt 49:593
28. Dou YS, Torralva BR, Allen RE (2003) J Mod Opt 50:2615
29. Gaussian 03, Revision C.02, Frisch MJ, Trucks GW, Schlegel HB, Scuseria GE, Robb MA, Cheeseman JR, Montgomery Jr. JA, Vreven T, Kudin KN, Burant JC, Millam JM, Iyengar SS, Tomasi J, Barone V, Mennucci B, Cossi M, Scalmani G, Rega N, Petersson GA, Nakatsuji H, Hada M, Ehara M, Toyota K, Fukuda R, Hasegawa J, Ishida M, Nakajima T, Honda Y, Kitao O, Nakai H, Klene M, Li X, Knox JE, Hratchian HP, Cross JB, Bakken V, Adamo C, Jaramillo J, Gomperts R, Stratmann RE, Yazyev O, Austin AJ, Cammi R, Pomelli C, Ochterski JW, Ayala PY, Morokuma K, Voth GA, Salvador P, Dannenberg JJ, Zakrzewski VG, Dapprich S, Daniels, AD, Strain MC, Farkas O, Malick DK, Rabuck AD, Raghavachari K, Foresman JB, Ortiz JV, Cui Q, Baboul AG, Clifford S, Cioslowski J, Stefanov BB, Liu G, Liashenko A, Piskorz P, Komaromi I, Martin RL, Fox DJ, Keith T, Al-Laham MA, Peng CY, Nanayakkara A, Challacombe M, Gill PMW, Johnson B, Chen W, Wong, MW, Gonzalez C and Pople JA (2004) Gaussian, Inc., Wallingford
30. Li X, Smith SM, Markevitch AN, Romanov DA, Levis RJ, Schlegel HB (2005) Phys Chem Chem Phys 7:233
31. Smith SM, Li X, Markevitch AN, Romanov DA, Levis RJ, Schlegel HB (2005) J Phys Chem A 109:5176

32. Fisher RA (1984) Optical phase conjugation. Academic, San Diego
33. Cheng LT, Tam W, Stevenson SH, Meredith GR, Rikken G, Marder SR (1991) J Phys Chem 95:10631
34. Cheng LT, Tam W, Marder SR, Stiegman AE, Rikken G, Spangler CW (1991) J Phys Chem 95:10643
35. Lascola R, Wright JC (1997) Chem Phys Lett 269:79
36. Lascola R, Wright JC (1998) Chem Phys Lett 290:117
37. Antoine R, Dugourd Ph, Rayane D, Benichou E, Broyer M, Chandezon F, Guet C (1999) J Chem Phys 110:9771
38. Kafafi ZH, Lindle JR, Pong RGS, Bartoli FJ, Lingg LJ, Milliken J (1992) Chem Phys Lett 188:492
39. Hebard AF, Haddon RC, Fleming RM, Kortan AR (1991) Appl Phys Lett 59:2109
40. Ritcher A, Sturm J (1995) Appl Phys A Mater Sci Process 61:163
41. Eklund PC, Rao AM, Wang Y, Zhou KA, Wang P, Holden JM, Dresselhaus MS, Dresselhaus G (1995) Thin solid films 257:211
42. Talapatra GB, Manickam N, Samoc M, Orczyk ME, Karna SP, Prasad PN (1992) J Phys Chem 96:5206
43. Matzuzawa N, Dixon DA (1992) J Phys Chem 96:6241
44. Weissn H, Ahlrichs R, Häser M (1993) J Chem Phys 99:1262
45. Shanker B, Applequist J (1994) J Phys Chem 98:6486
46. Van Gisbergen SJA, Snijders JG, Baerends EJ (1997) Phys Rev Lett 78:3097
47. Jonsson D, Norman P, Ruud K, Å gren H, Helgaker T (1998) J Chem Phys 109:572
48. Machon M, Reich S, Thomsen C, Sanchez-Portal D, Ordejon P (2002) Phys Rev B 66:155410
49. Matzuzawa N, Dixon DA (1992) J Phys Chem 96:6241
50. Weiss H, Ahlrichs R, Häser M (1993) J Chem Phys 99:1262
51. Bonin KD, Kresin VV (1997) Electric-dipole polarizabilities of atoms, molecules, and clusters. World Scientific, Singapore
52. Hu YH, Ruckenstein E (2005) J Chem Phys 123:214708